



## RAPD Analysis, Synthesis of Zinc Oxide Nanoparticles Derived from *Aerva lanata* Flower: Characterization and Antimicrobial Screening

THAMARASELVI GANESAN<sup>1,✉</sup>, SURIYAVATHANA MUTHUKRISHNAN<sup>1,\*</sup>, BRAIVY ANTO<sup>1,✉</sup>,  
MANIKANDAN MATHAIYAN<sup>1,✉</sup>, SOBIYA PRADEEP KUMAR<sup>1,✉</sup>, R. JAYAPRAKASH<sup>2,✉</sup> and M. SUGANYA<sup>3,✉</sup>

<sup>1</sup>Plant Therapeutics Laboratory, Department of Biochemistry, School of Bioscience, Periyar University, Salem-636011, India

<sup>2</sup>Department of Chemistry, School of Arts and Science, AV Campus, Vinayaka Mission's Research Foundation (Deemed University), Paiyanoor, Chennai-603104, India

<sup>3</sup>Department of Biochemistry, Islamiah Women's Art's and Science College, Vaniyambadi-635751, India

\*Corresponding author: E-mail: suriyaveda@periyaruniversity.ac.in

Received: 28 May 2023;

Accepted: 11 July 2023;

Published online: 31 August 2023;

AJC-21357

Nanoparticles and plant phytochemicals are receiving great interest between materials and drug discovery studies. Hence, this work report the synthesis of zinc oxide nanoparticles (ZnO NPs) using Pashanabheda (*Aerva lanata*), which is employed as an antiurolithiatic agent. The selection of the *Aerva lanata* flower, a member of the Amaranthaceae family, as the source material was based on its ability to exhibit a wide range of genetic modifications in response to various environmental and geographical factors. The synthesized ZnO NPs were characterized by UV, FTIR, XRD and scanning electron microscopy. Due to flower's chemical make-up and presence of several functional groups in ZnO nanoparticles were found to be effective at bio-reduction and capping. Antibacterial assay against *B. subtilis*, *S. aureus*, *K. pneumonia* and *Pseudomonas* using ZnONPs of *A. lanata* flower exhibited excellent inhibition zones between 11 mm and 18 mm for 100 µg/mL.

**Keywords:** *Aerva lanata*, RAPD analysis, Green synthesis, ZnO nanoparticle, Antibacterial activity.

### INTRODUCTION

Different kinds of illnesses have been treated with medicinal plants from different parts of the world. Medicinal plants have a wide range of phytochemical substances with potential pharmaceutical use [1]. Likewise, more and more drug-resistant strains of bacteria and fungi have emerged in recent years [2]. Herbal remedies have long been relied upon for their curative effects and are a staple of traditional medicines, which are an important source of novel medications [3-6]. But, the plants DNA sequences are differed based on the soil nature and the regions. To measure the variation, recent biotechnology field is using Random Amplified Polymorphic DNA (RAPD) analysis. One of the key benefits of RAPD is that it does not required DNA pre-sequencing. Accessions have been named and categorized using RAPD analysis, among other applications [7].

*Aerva lanata*, a rare member of the Amaranthaceae family, is utilized in local medicine under the names Kalluruvi and Pongal poo. The phytochemical components of medicinal plants

like *A. lanata* are used to treat and cure human illnesses; these components are non-phytotoxic and biodegradable [8]. The prostrate perennial shrub *Aerva lanata*, commonly known as mountain knot grass, is native to the mountain plains of diverse regions in India [9]. *A. lanata* flowers have been found to possess many biological activities, including anti-urolithiatic, anti-diabetic, analgesic, anti-inflammatory, diuretic and antiasthmatic properties [10-13]. The therapeutic capabilities of plants are attributed to the presence of bioactive secondary chemicals. In order to determine the scientific foundation for their use and to discover new or potent compounds for treating a variety of human diseases, it is crucial to maintain these medicinal plants [14].

Nanomaterials have had far-reaching implications on civilization as crucial building blocks of nanotechnology due to various applications in chemistry, biotechnology and drug discovery field [15]. Nanomaterials are made up of atoms and molecules on a billionth-of-a-metre scale. This is due to their expanded surface area and distinctive size [16,17]. The present study incorporated the findings from RAPD analysis, ZnO nano-

particles and their antibacterial activity reports in its investigation. The present work utilized RAPD analysis as a method to evaluate the genetic diversity of *A. lanata*. The plant samples were collected from various geographical zones and carried for the studies. The flower with the highest RAPD intensity was selected for the synthesis of ZnO nanoparticles in an aqueous media. In addition, the prepared nanomaterial was characterized and also investigated its bacterial inhibition efficacy [18-20].

## EXPERIMENTAL

**Collection of samples:** Fresh *A. lanata* plants were collected from four different zones such as Sathyamangalam, Trichy, Pondicherry and Dharmapuri cities and authenticated by Department of Botany, Periyar University, Salem, India.

**Sample preparation for genetic variation:** The collected fresh *A. lanata* plants were cleaned with double-distilled water and stored in moisture free plastic bags.

**Genetic variation by RAPD analysis of *A. lanata* flower:** Numerous fields, including gene mapping, population genetics, molecular evolutionary genetics, plant and animal breeding can benefit from the use of RAPD markers. This is mostly due to the method's superior ability to produce a large number of markers rapidly, inexpensively and efficiently as compared to older techniques. The DNA finger printing approach known as RAPD, which reveals genetic variants at DNA sequence level that differs from evolutionary causes such DNA deletion, addition, replacement, repetition and translocation. High yields of clean DNA samples are required for the genetic study of plants. The RAPD analyses of collected *A. lanata* flower from various areas were investigated by known standard procedure [21].

**Preparation of zinc oxide nanoparticles using *A. lanata* flower:** A mixture of 0.1 mM of zinc nitrate and 25 g of dried powdered *A. lanata* flower (high intensity Sathyamangalam sample) were diluted in 500 mL of distilled water for the synthesis of zinc oxide nanoparticles and then heated to 100 °C in a boiling water bath for 80 min. The reaction mass temperature was allowed to cool at room temperature and filtered. The filtrate portion was washed by excess of water and diluted in double distilled water. The fluid was centrifuged for 15 min at a speed of 3000-4000 rpm. Following centrifugation, the supernatant was discarded in order to extract the pellet, which was then separated and put into a petri plate with a small amount of supernatant. The remaining samples were preserved in a tightly packed bottle in the dark room for three weeks. The pellet of ZnO NPs was then dried in a hot air oven and conserved in airtight bottles for further analysis.

Similarly, the ZnO NPs were also prepared from the other samples collected from the different region.

**Absorption study:** The UV-Vis spectrum was recorded on the nano drop-8000 UV-Vis spectrophotometer between 200 and 700 nm wavelength range in order to monitor the bio-reduction of zinc nitrate periodically in the the floral extracts of *A. lanata* [22].

**FTIR analysis:** FTIR spectral analysis of the biosynthesized ZnO NPs reveals the presence of potential biomolecules which are accountable for the stability and reduction of the

biosynthesized ZnO NPs in the range of 4000-400  $\text{cm}^{-1}$  using Perkin-Elmer Spectrum-2000 FTIR instrument.

**XRD analysis:** The crystal lattice of the biosynthesized ZnO NPs was studied using XRD patterns. The XRD pattern obtained from the drop-coated ZnO nanoparticles on a glass substrate revealed a broad range of Bragg's angle  $2\theta$ . The XRD analysis was conducted at a scanning rate of  $2^\circ/\text{min}$  using ULTIMA IV-X-ray powder diffractometer, RIGAKU Ltd., Japan using Cu radiation source.

**SEM analysis:** The ZnO NPs were synthesized and subsequently subjected to scanning electron microscopy (SEM) analysis. A cover slip was used during the imaging process to collect the images. The images themselves contained information about the voltage utilized, the magnifying glass employed, and the overall size of the contents.

**Antibacterial activity:** The standard agar well diffusion method was successfully used to test the antibacterial activity of the phytochemicals incorporated zinc oxide nanoparticles (ZnO NPs) of *A. lanata* against *Staphylococcus aureus*, *Bacillus subtilis*, *Klebsiella pneumonia* and *Pseudomonas bacteria* [23,24]. Subsequently, the plates underwent thorough examination and then zones of inhibition (ZOI) against several types of microorganisms were quantified.

## RESULTS AND DISCUSSION

The degree of polymorphism can be measured for the genetic fingerprints of *A. lanata* flower by RAPD markers. Four plants of *A. lanata* collected from different places have chosen RAPD analysis and compared with genomic DNA with 1 primer (PGF04). The results exposed that the similar in morphology and easily adulterated (Fig. 1). The wide geographical and climatic distribution is an indication that there exists a tremendous genetic diversity in the *A. lanata* flower. Hence, it needs to be identified hence the focus of this study is on the genetic diversity and

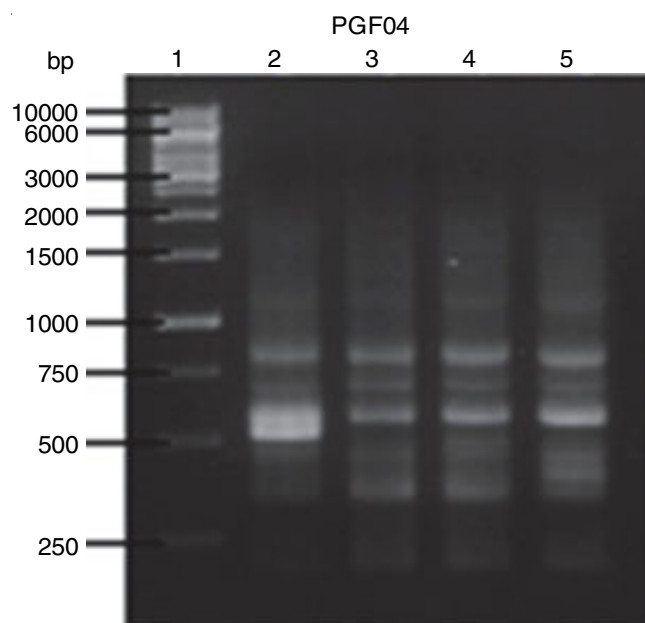


Fig. 1. RAPD analysis results (1). Lane 1 - 1kbDNA ladder, (2). Lane 2 - Sathyamangalam, (3). Lane 3 - Pondicherry, (4). Lane 4 - Dharmapuri and (5). Lane 5 - Trichy carried out with "Primer: PGF04"

relationship. When compared the geographical distribution, namely Sathyamangalam, Trichy, Pondicherry and Dharmapuri districts, the plant source obtained from the Sathyamangalam zone has been observed to possess significant activity [25]. The Sathyamangalam sample was collected in order to facilitate the subsequent synthesis of ZnO nanoparticles.

**UV-visible studies:** The absorption characteristic of zinc oxide nanoparticles (ZnO NPs) was observed, when it was extracted from *A. lanata* flower. The significant absorbance peak was identified by UV-visible spectrophotometer analysis and was connected to the surface plasmon resonance of Zn nanoparticles (Fig. 2). An observed absorption at 338.7 nm is coincidence with reported value [20]. The energy gap was detected at 2.69 eV for the biosynthesized ZnO NPs. The plant extract simultaneously serves as a stabilizing and reducing agents. ZnO nanoparticles only have one peak in the spectrum, appeared at 340 nm. The bioreduction and capping may be caused due to the presence of several bioactive chemicals and their functional groups present in the flower extract [20].

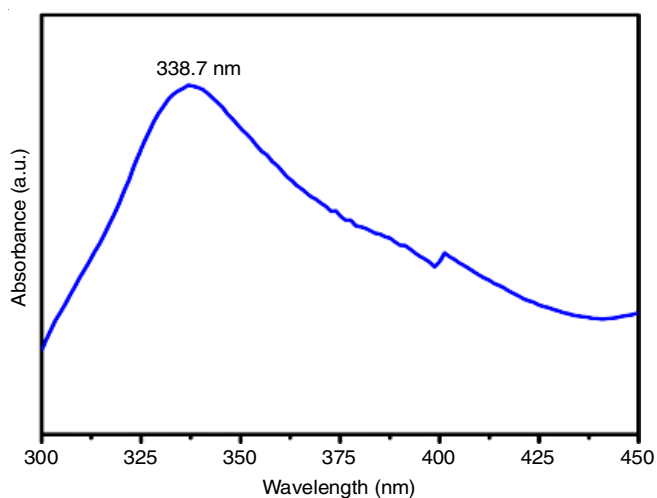


Fig. 2. UV-Vis spectrum of biosynthesized ZnO NPs from *A. lanata*

**FTIR studies:** The FT-IR technique exerts an influence on the composition and evolution of functional groups present in the biosynthesized ZnO nanoparticles. Moreover, it can be inferred that the development of ZnO NPs is attributed to the interactions among phenolic compounds, alkynes, terpenoids, and flavonoids. Thus by using FTIR analysis, the potential functional group involved in reducing  $Zn^{2+}$  ions to  $Zn^0$  was identified in the *A. lanata* flower extract. A peak at  $3428.91\text{ cm}^{-1}$  reveals the N-H stretching vibrations of amine, similarly the peak at  $2922.41\text{ cm}^{-1}$  the reveals CHO stretching vibrations of aldehyde (Fig. 3). The C-H stretching vibrations of alkane was observed at  $1652.13\text{ cm}^{-1}$ , while the C=O stretching vibrations of aromatic and carboxylic acid's COOH stretching vibrations were revealed at  $1410.27$  and  $1245.53\text{ cm}^{-1}$  respectively. The details of the other important peaks appeared in the FTIR spectrum are listed in Table-1.

**XRD studies:** Likewise, X-ray diffraction (XRD) analysis exposed several distinctive diffraction peaks (Fig. 4) such as the sharp and narrow peak at  $20.18^\circ$ ,  $24.03^\circ$ ,  $30.14^\circ$ ,  $47.51^\circ$ ,  $49.65^\circ$ ,  $52.36^\circ$ ,  $64.83^\circ$ ,  $68.26^\circ$ , which were assigned to (002),

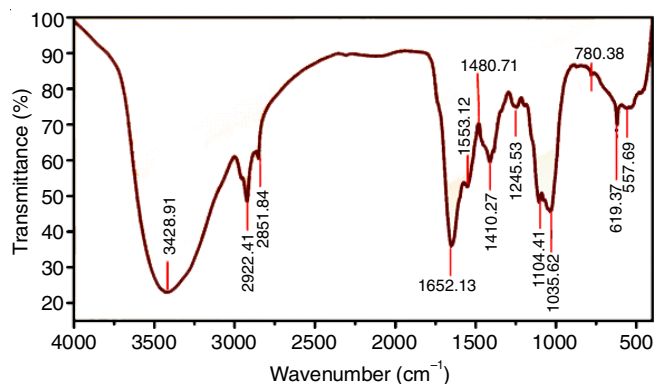


Fig. 3. FTIR spectrum of biosynthesized ZnO NPs from *A. lanata*

TABLE-1  
FTIR VIBRATIONAL PEAKS OF BIOSYNTHESISED  
ZnO NPs FLOWER EXTRACT OF *A. lanata*

Peak	Frequency range ( $\text{cm}^{-1}$ )	Bonds	Compound type
P1	3428.91	N-H	Primary amine
P2	2922.41	CHO	Aldehyde
P3	2851.84	C-H	Alkane
P4	1652.13	C=O	Aromatic ketones
P5	1553.12	N-H	Amine primary
P6	1410.27	COOH	Carboxylic acid
P7	1245.53	COOH	Carboxylic acid
P8	1104.41	O-H	Secondary alcohol
P9	1035.62	=C-O-C	Ether
P10	780.38	C=C	Aromatic-mono-substituted
P11	619.37	C-C-N	Nitriles
P12	557.69	C-C-N	Nitriles

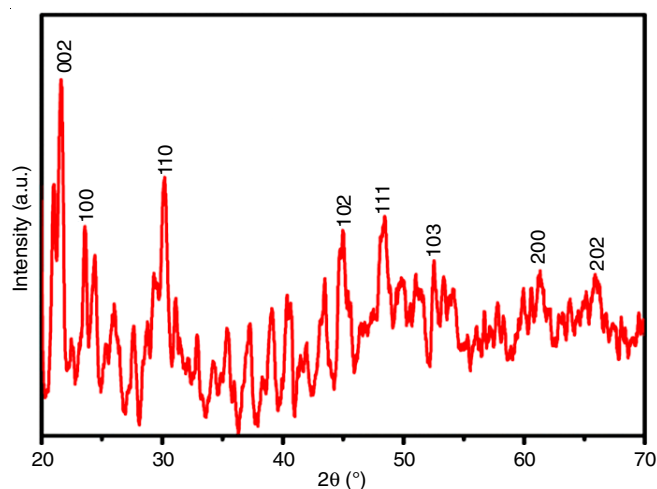


Fig. 4. XRD spectrum of biosynthesized ZnO NPs from *A. lanata*

(100), (110), (102), (111), (103), (200), (202), respectively. The facets of characteristics of cubic centred of ZnO nanoparticles face centered cubic (FCC) crystal structure were used to index the planes (JCPDS card No. 36-1451). The diffraction peaks, which are sharp and thin, appear at about  $2\theta$  of  $47.51^\circ$ ,  $51.20^\circ$  and  $74.83^\circ$  were assigned to (111), (200) and (220) plane values of ZnO nanoparticles.

**Morphological studies:** A high resolution SEM images (Fig. 5a-b) of biosynthesized ZnO NPs produced from *A. lanata* flower extract confirmed the existence of nanosize particles.

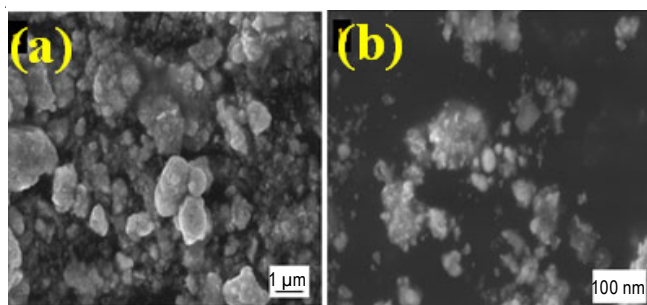


Fig. 5. SEM images of biosynthesized ZnO NPs from *A. lanata*

The crystals primarily exhibited spherical, cuboidal and irregular polydispersity, forming large formations characterized by distinct structural features. The observed surfaces such as cuboidal and spherical sizes of ZnO NPs were found to be the range from 66.77 to 117.2 nm.

**Biological studies:** The antibacterial properties of biosynthesized ZnO NPs were evaluated against several pathogens such as *Bacillus subtilis*, *Staphylococcus aureus*, *Klebsiella pneumonia* and *Pseudomonas*. For both positive and negative controls, as well as serially diluted concentrations such as 25, 50, 75 and 100 µg/mL of ZnO NPs were subjected for the inhibition study. Table-2 shows the inhibition zones (in mm) formed around the nanoparticles and positive control (neomycin antibiotic). The maximum inhibited area were observed as 18 mm against *B. subtilis*, 11 mm against *S. aureus*, 12mm against *K. pneumonia* and 14 mm against *Pseudomonas* for maximum concentration of 100 ppm.

Pathogens	Concentration (µg/mL)/ Inhibition zone (mm)				Standard
	25	50	75	100	
<i>B. subtilis</i>	4	7	9	18	19
<i>S. aureus</i>	3	5	8	11	21
<i>K. pneumonia</i>	5	6	8	12	21
<i>Pseudomonas</i>	4	8	11	14	19

## Conclusion

The genetic diversity of *Aerva lanata* was assessed using RAPD analysis, and it was determined that the sample taken from the Sathyamangalam district exhibited the highest level of significance. Moreover, the antimicrobial efficacy of zinc oxide nanoparticles (ZnO NPs) was reported to be effective against all bacterial strains tested.

## ACKNOWLEDGEMENTS

First author is deeply grateful to all Co-authors for the success of this research outcomes.

## CONFLICT OF INTEREST

The authors declare that there is no conflict of interests regarding the publication of this article.

## REFERENCES

1. A. Sofowora, E. Ogunbodede and A. Onayade, *Afr. J. Tradit. Complement. Altern. Med.*, **10**, 210 (2013); <https://doi.org/10.4314/ajtcam.v10i5.2>
2. B. Aslam, W. Wang, M.I. Arshad, M. Khurshid, S. Muzammil, M.H. Rasool, M.A. Nisar, R.F. Alvi, M.A. Aslam, M.U. Qamar, M.K.F. Salam and Z. Baloch, *Infect. Drug Resist.*, **11**, 1645 (2018); <https://doi.org/10.2147/IDR.S173867>
3. S.T. Appapalam and R. Panchamoorthy, *J. Taiwan Inst. Chem. Eng.*, **78**, 539 (2017); <https://doi.org/10.1016/j.jtice.2017.06.035>
4. M. Ekor, *Front. Pharmacol.*, **4**, 177 (2013); <https://doi.org/10.3389/fphar.2013.00177>
5. N.A. Al-Dhabi, A.-K. Mohammed Ghilan, G.A. Esmail, M. Valan Arasu, V. Duraipandiyar and K. Ponnurugan, *J. Infect. Public Health*, **12**, 549 (2019); <https://doi.org/10.1016/j.jiph.2019.01.065>
6. M.V. Arasu, S. Arokiyaraj, P. Viayaraghavan, V. Duraipandiyar, T.S.J. Kumar, N.A. Al-Dhabi and K. Kaviyarasu, *J. Photochem. Photobiol. B*, **190**, 154 (2019); <https://doi.org/10.1016/j.jphotobiol.2018.11.020>
7. S. Fukuoka, K. Hosaka and O. Kamijima, *Jpn. J. Genet.*, **67**, 243 (1992); <https://doi.org/10.1266/jjg.67.243>
8. A. Nostro, M.P. Germandò, V. Dangelo, A. Marino and M.A. Cannatelli, *Lett. Appl. Microbiol.*, **30**, 379 (2000); <https://doi.org/10.1046/j.1472-765x.2000.00731.x>
9. M.A. Goyal, B. Pareek, P. Nagori and D. Sasmal, *Pharmacogn. Rev.*, **5**, 195 (2011); <https://doi.org/10.4103/0973-7847.91120>
10. N. Silvia, C.H. Rajeswari, D. Mounica, R. Manasa and D. Prasanth, *Pharmacogn. J.*, **6**, 29 (2014); <https://doi.org/10.5530/pj.2014.5.6>
11. A. Pieczykolan, W. Pietrzak, U. Gawlik-Dziki and R. Nowak, *Molecules*, **26**, 3486 (2021); <https://doi.org/10.3390/molecules26123486>
12. E.O. Sousa and J.G.M. Costa, *Brazil. J. Pharmacogn.*, **22**, 1155 (2012); <https://doi.org/10.1590/S0102-695X2012005000058>
13. M. Goyal, B.P. Nagori, A. Pareek and D. Sasmal, *Pharmacogn. Rev.*, **5**, 195 (2011); <https://doi.org/10.4103/0973-7847.91120>
14. D. Karou, A. Savadogo, A. Canini, S. Yameogo, C. Montesano, J. Simporé, V. Colizzi and A.S. Traore, *Afr. J. Biotechnol.*, **5**, 195 (2006); <https://doi.org/10.4314/ajb.v4i12.71463>
15. M. Ijaz, M. Zafar and T. Iqbal, *Inorg. Nano-Metal Chem.*, **51**, 744 (2021); <https://doi.org/10.1080/24701556.2020.1808680>
16. K.S.B. Naidu, *Curr. Trends Biotechnol. Pharm.*, **14**, 111 (2020); <https://doi.org/10.5530/ctbp.2020.1.11>
17. S. Saiganesh, T. Krishnan, G. Narasimha, H. Almoallim, S. Alhari, L. Reddy, K. Mallikarjuna, A. Mohammed and V. Prabhakar, *Crystals*, **11**, 124 (2021); <https://doi.org/10.3390/cryst11020124>
18. A. Venkatesan, J.V.R. Antony Samy, R.R. Anantha Sayanam, J. Rajendran and V. Natesan, *Asian J. Chem.*, **33**, 1736 (2021); <https://doi.org/10.14233/ajchem.2021.23237>
19. S. Duraisamy, N. Vijayakumar, J. Rajendran, A. Venkatesan, B. Kartha, S.P. Kandasamy, M. Nicoletti, N.S. Alharbi, S. Kadaikunnan, J.M. Khaled and M. Govindarajan, *J. Drug Deliv. Sci. Technol.*, **69**, 103160 (2022); <https://doi.org/10.1016/j.jddst.2022.103160>
20. N. Vijayakumar, V.K. Bhuvaneshwari, G.K. Ayyadurai, R. Jayaprakash, K. Gopinath, M. Nicoletti, S. Alarifi and M. Govindarajan, *Saudi J. Biol. Sci.*, **29**, 2270 (2022); <https://doi.org/10.1016/j.sjbs.2021.11.065>
21. N. Kumari and T. Saroj Kumar, *Am. J. Anim. Vet. Sci.*, **9**, 6 (2014); <https://doi.org/10.3844/ajavsp.2014.6.13>
22. S. Palithya, S.A. Gaddam, V.S. Kotakadi, J. Penchalani, N. Golla, S.B.N. Krishna and C.V. Naidu, *Parti. Sci. Tech.*, **55**, 14 (2021); <https://doi.org/10.1080/02726351.2021.1919259>
23. M. Suriyavathana and M. Punithavathi, *Int. J. Adv. Res. Sci. Eng.*, **6**, 526 (2017).
24. A. Jayachandran, T.R. Aswathy and A.S. Nair, *Biochem. Biophys. Rep.*, **26**, 100995 (2021); <https://doi.org/10.1016/j.bbrep.2021.100995>
25. A. Praveena and M. Suriyavathana, *Asian J. Pharm. Clin. Res.*, **6**, 148 (2013).